High Energy Physics and Nuclear Physics

Volume 21, Number 3

Atmospheric Cherenkov Telescope

Jiang Yinlin, Chen Yongzhong, Xu Chunxian, He Huilin,
He Huihai, Li Huidong, and Huo Anxiang

(Institute of High Energy Physics, The Chinese Academy of Sciences, Beijing, China)

Two tracking atmospheric Cherenkov telescopes have been operated at the Xing Long Station, Beijing Astronomical Observatory, for the observation of atmospheric Cherenkov radiation produced by extensive air showers. They are used to search for point sources of very high energy (VHE) gamma-rays and to study their emission characteristics as well as to detect the spatial distribution of VHE gamma-ray intensity. The structure and the performance of the telescopes as well as the testing results under observation conditions are presented in this paper.

Key words: atmospheric Cherenkov radiation, telescope, very high energy gamma-rays, gamma-ray source, gamma-ray astronomy.

1. INTRODUCTION

The VHE gamma-ray astronomy is an important part of full wavelength band astronomy and a link between space high energy gamma-ray ($\lesssim$ 30 GeV) detection and ground-based ultra high energy (UHE, 10^{14}-10^{16}eV) gamma-ray detection [1-3]. It concerns photons with energy of 10^{11}-10^{13}eV. Because of the very weak flux of VHE gamma-rays, in the foreseeable future there will be no satellite-borne detectors that can be fully competent to the detection of gamma-rays with such a high energy and weak flux. However, when a gamma-ray enters the atmosphere, it induces extensive air showers (EAS) by electromagnetic cascade processes. The bulk of electrons and positrons produced in an EAS emit Cherenkov photons, which are in a cone with an axis directed to the same direction of the incident VHE gamma-ray. The cone covers an area with a radius of 100-150 m at a lower elevation. These Cherenkov photons produced by an EAS form a fast pulsed flow of photons, which

Received on July 4, 1996.

distribute in the cone uniformly and last a very short time (10 ns) with a small angular divergence (1°). Therefore a local detector not only held a very large sensitive area to detect an incident VHE gamma-ray but also has the capability to determine its direction by measuring the flow orientation. The true atmospheric Cherenkov event can be extracted from the bulk background noise by means of fast coincidence between signals of several detectors. So far the atmospheric Cherenkov technique is the only applied method in the VHE gamma astronomy [4-8].

By developing and improving the atmospheric Cherenkov telescope, a great progress has been made in the field of VHE gamma-ray astronomy. It has been confirmed that Crab Nebula, Vela Nebula, and PSR1706-44 are VHE gamma-ray sources in our Galaxy [9,10], and an active galactic nucleus, named Mark421, is an extragalactic VHE gamma-ray source [10-12]. The existence of VHE gamma-ray sources indicates that there are high energy (HE) objects and HE processes in the universe. A VHE gamma-ray source should be a cosmic particle source too. As with the other new windows of astronomy, in the wavelength band of VHE gamma-ray astronomy there should be more new phenomena and discoveries.

For the observation and study of VHE gamma-ray astronomy, two tracking Cherenkov telescopes (named ACT-2 and ACT-3) have been installed at the Xing Long Station (40°23.6′N; 117°34.6′E; 960 m a.s.l.), Beijing Astronomical Observatory (BAO) by an internal collaboration between IHEP and BAO, the Chinese Academy of Sciences. They are used to search for point sources of VHE gamma-rays and to study their emission characteristics as well as detect the space distribution of VHE gamma-ray intensity. As the Xing Long Station has very good geographical and weather conditions for optical astronomical observation, it is an ideal site for VHE gamma-ray observation.

2. STRUCTURE AND PERFORMANCE OF THE TELESCOPE

The two atmospheric Cherenkov telescopes (ACT-2 and ACT-3) installed at the Xing Long Station have the same structure and performance. Each telescope is comprised of a computer (PC-386) -steered alt-azimuth platform, a servo tracking system, collecting light mirrors, light sensor detectors, fast electronics circuits, recording and timing system, etc. Figure 1 shows the outward appearance of the tracking alt-azimuth platform, collecting light mirrors, and the light sensor detectors (PMs).

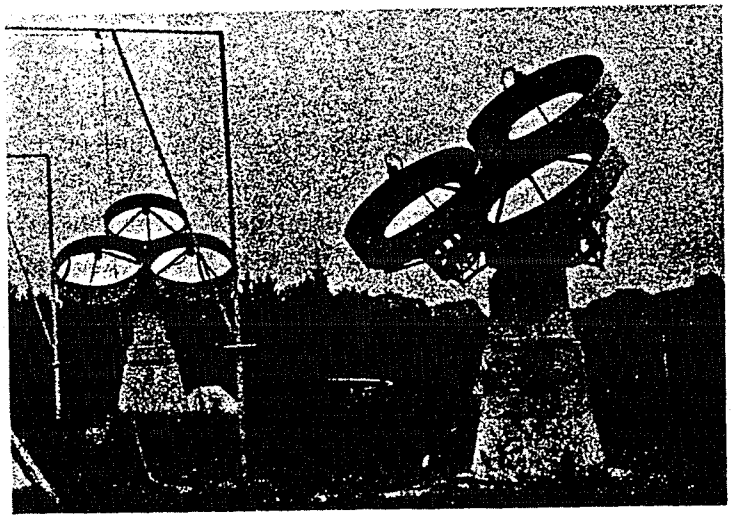

ACT-2 ACT-3

Fig. 1
The outward appearance of the Cherenkov telescopes ACT-2 and ACT-3.

2.1. Tracking alt-azimuth platform and the servo tracking system

To track a celestial object, a computer-steered alt-azimuth platform and a servo tracking system were employed. Two shafts, two optical shaft encoders of 14 digits, and a drive motor were used to control the platform at its altitude and azimuth individually. The optical shaft encoders have the real pointing (altitude and azimuth) of the telescope and make a real-time data transmission onto the servo controlling system. The data are displayed on the board of a Nixie tube with an accuracy of 0.02°. The servo tracking system is controlled by a PC-386, which takes out the standard Beijing time from the timing system every minute, calculates the direction of the aim object and compares the real direction of the telescope with the calculated direction of the tracked object. If the difference between the two directions is greater than 1 digit (0.02°) of the optical shaft encoder, the servo controlling system will give out a proper drive current based on the value of the difference to make the telescope point at the object.

The alt-azimuth platform is equipped with a paraxial finder, which is used to calibrate the zero point of altitude and azimuth based on the positions of the polestar and some bright stars near the transit in the field of view of the finder. When the Cherenkov telescope tracks different bright stars individually, the tracking accuracy can be obtained by the finder. The measured tracking accuracy is better than 0.1°. Our Cherenkov telescope can track a star with an altitude greater than 20°.

2.2. Collecting mirror and light sensor detector

The optical system of the Cherenkov telescope is comprised of three paraxial, parabolic searchlight mirrors of 1.5 m diameter mounted on a computer-steered alt-azimuth platform. The mirror is made of polished glass with an average thickness of 15 mm and back coated with the silver layer

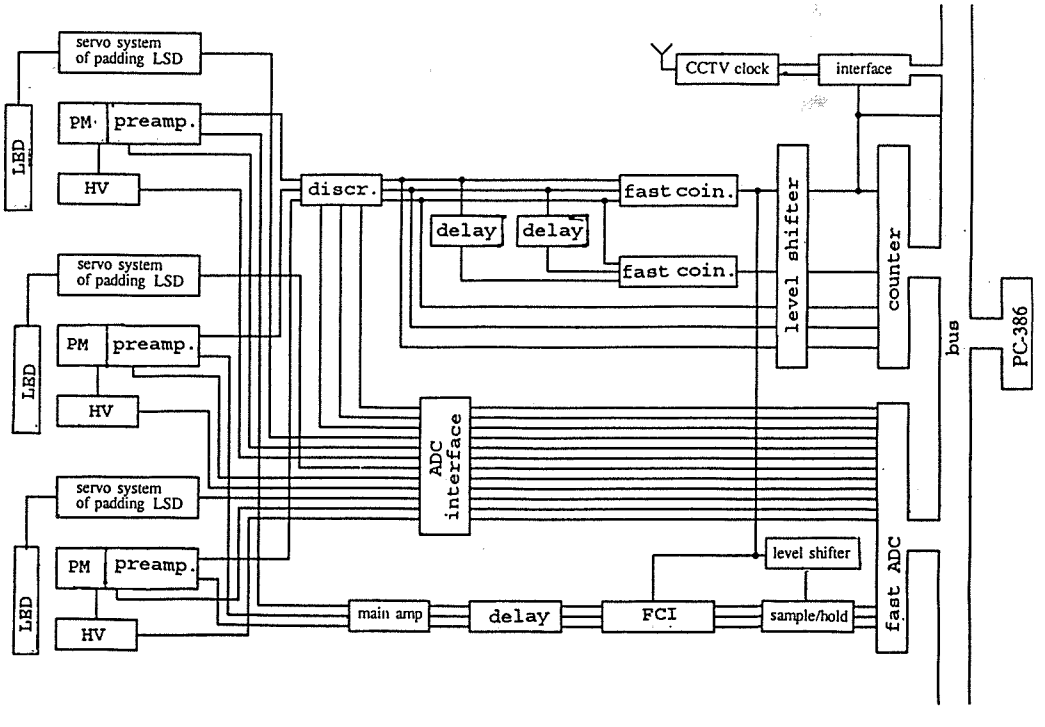

Fig. 2
The block diagram of the fast electronics and recording and timing system.

and protective layer. The mirror with a focal length of 639 mm has an average reflectivity of 0.5 for the atmospheric Cherenkov light wave band. The vertical axis of the tracking platform is parallel to the common axis of the three paraxial search light mirrors within 0.05°. The focus position of the searchlight mirror has been determined by the position of the polestar's spot on the focal plane with radial offset smaller than 0.05°.

The detector, measuring the pulsed photon flux of the atmospheric Cherenkov radiation, consists of a magnetic shielding fast photomultiplier (XP-2020) and a fast preamplifier with a gain of 10 mainly comprised of a hybrid amplifier VV-100B. The cathode of the PM is placed coaxially at the focal plane of the mirror. An adjustable circular aperture is placed closely at the front of the cathode defining a geometrical field of view. By adjusting the brightness of the light emitting diode (LED) mounted near the cathode of the PM, a servo anode current compensation circuit is used to stabilize the anode current against the effects of the celestial brightness and the weather.

2.3. Fast electronics and data acquisition system

The block diagram of the fast electronics and data acquisition system is shown in Fig. 2. Two similar pulse signals are output by a fast preamplifier of the PM detector. One is used to measure the amplitude of the pulse. This pulse signal is amplified by a main amplifier and shaped by a fast current integrator (FCI) and delayed 50 ns before FCI. Another signal is put into a discriminator, which then outputs three standard signals of the NIM level when the input pulse is greater than 30 mV. The width of the NIM signal is 10 ns. One of the NIM signals is used to yield the Cherenkov event trigger by a three-fold coincidence. When the trigger comes, the arrival time of the event and amplitudes of three pulses are recorded, and the event number, arrival time, and three amplitudes are displayed on the computer screen. The second signal of the discriminator is put into another three-fold coincidence after being delayed with different times (0, 33 ns, 66 ns). This coincidence rate is used as a measurement of the accidental coincidence rate. The third signal of the discriminator is used to measure the individual detector rate.

To monitor the stability of every part of the system, the pointing direction (azimuth and elevation) of telescope, high voltages and anode currents of PMs, currents of padding LED, thresholds of discriminators, individual detector rates, event counting rate, and accidental counting rate are each recorded every minute and displayed on the computer screen. The data acquisition and the tracking control are completed by the same computer PC-386.

2.4. Timing system

In order to study the periodic VHE gamma-ray emission of a millisecond pulsar, it is necessary to measure the event arrival time accurately. A timing system with a high accuracy was developed by the Chinese National Institute of Metrology, which consists of a local oven-stabilized crystal clock offering a fundamental frequency with trimmability and a TV standard time and frequency signal demodulator. By synchronizing the leading edge of the second pulse of the local clock with that of the TV standard Beijing time, the bias of two leading edges is shown to be within 200 ns. Monitoring the time drift of the local clock and adjusting the fundamental frequency of the local clock continuously, the difference between the local clock and the Beijing standard time is less than 2 μs. Because the accuracy of the CCTV-1 standard Beijing time is ± 3 μs and the local clock puts out the BCD code from one hour to 1 μs, the resolution of the arrival time is 1 μs, and its absolute accuracy is better than ± 20 μs.

3. MAIN PERFORMANCES

The accompanied atmospheric Cherenkov radiations of isotropic cosmic particle-initiated showers are very similar to that of VHE gamma-ray-initiated showers, which cause a background for VHE

gamma-ray observation. To decrease the background, it better to acquire a smaller aperture for the telescope. On the other hand, because the Cherenkov radiation has a divergence of about 1°, to collect more Cherenkov photons the aperture cannot be small. With both these factors in mind, a circular aperture of 1.5 cm radius should be taken, which defines the full geometrical field of view to be 1.35°.

Because of the very weak pulse signal of atmospheric Cherenkov radiation, the PM must have a large enough gain, and at the same time it must maintain a safe anode current. So the Cherenkov telescope has to operate on a clear and moonless night. A proper high voltage for XP-2020 is selected in order to keep the anode current in the range of 4-6 μA. The padding lamp circuit maintains an anode current of 7.5 μA to ensure the gain of the PM being constant. Under the above-mentioned condition, the main performance is as follows.

3.1. Dependence of altitude

On a clear and moonless night, the single channel rate is about 3-10 kHz for the three light sensor detectors. The bulk among them are noise. As a three-fold coincidence of the three channels, signals provide an almost accident-free detection of a Cherenkov signal. The probability of accident coincidence of the three channels is about 10^{-3}. The rate of three-fold coincidence is 20-60 per minute, which depends on the weather conditions and the altitude pointed at by the telescope.

Figures 3(a) and 3(b) show the rate as a function of the time while ACT-2 and ACT-3 track the Crab Pulsar. Figure 3(c) shows the altitude Z as a function of the time. It is seen from Fig. 3 that the rate depends on the altitude Z obviously, which obeys a relation of $N_0\cos^n(Z)$, where N_0 is the rate pointing to the zenith. Our experiments gave out that N_0 is in the range of 30-60 and n in 2-3. The values are changed with season, weather, and the threshold energy.

3.2. Decoherence curve

The two telescopes, ACT-2 and ACT-3, are separated by 11.5 m. When they simultaneously track the same celestial object, it is found that the bulk of events have exactly the same arrival time in the two data sets recorded by ACT-2 and ACT-3. This means that the two telescopes always measure the same event of atmospheric Cherenkov radiation, the so-called coherent event. Obviously the number of coherent events is related to the angle between the two axes, the property of optical systems of the two telescopes, the pointing accuracy, the divergence of atmospheric Cherenkov radiation, etc.

When the axis of ACT-3 holds a fixed point to the zenith and ACT-2 points to directions with different zenith distance (0, $\pm$0.11, $\pm$0.29, ..., $\pm$2.0°) the coincidence rate N_C per minute is measured. N_C changes with the angle between the two telescope axes. By this procedure the decoherence curve is obtained and shown in Fig. 4. From Fig. 4, it is seen that the decoherence curve has only $-0.03°$ offset, and with rather good symmetry which indicates the mounting and the alignment of the tracking systems of the two telescopes are as good as expected. The full width of half maximum (FWHM) of the decoherence curve is 1.7°, greater than the full geometric field of view (1.35°). In general, under a pretty good optical system this is caused mainly by the divergence (about 1°) of atmospheric Cherenkov radiation. The resulting decoherence curve, shown in Fig. 4, is consistent with either the simulated result [13] or some measured results by similar telescopes [14,15].

3.3. Detecting efficiency and threshold energy

The detection of Cherenkov light pulses includes many statistical processes. Under the first approximation, the density of Cherenkov photons is proportional to the primary energy. Therefore the detecting efficiency should relate to the primary energy and the threshold energy of the telescope. When ACT-2 and ACT-3 point to the zenith simultaneously, N_2 and N_3 are the total numbers of the

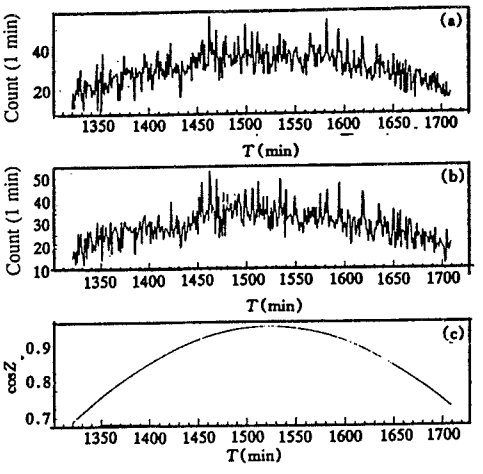

Fig. 3
Under tracking of the Crab Pulsar, (a) the rate of ACT-2 as a function of the time; (b) the rate of ACT-3 as a function of the time; and (c) the tracking altitude Z as a function of the time.

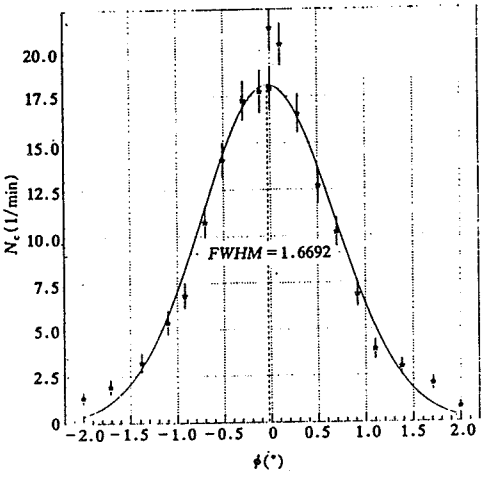

Fig. 4
Decoherence curve between ACT-2 and ACT-3.

event recorded by ACT-2 and ACT-3 individually in the same period, and N_{23} represents the number of coherent events. So $\eta_r = N_{23}/N_3$ is the relative integrated detection efficiency of ACT-2 to ACT-3 above the threshold energy of ACT-3, and N_{23}/N_3 has a similar meaning. Figure 5 shows the η_r as a function of the event amplitude A output by the premultiplier, where A corresponds to the primary energy. When the event amplitude A is greater than 0.1 V, the η_r is larger than 98%.

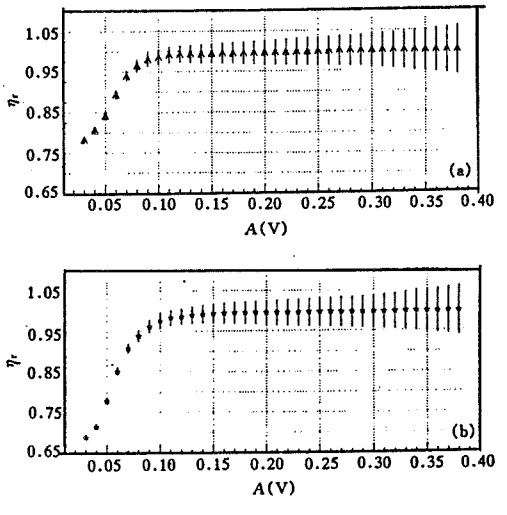

Fig. 5
The relative integrated efficiency as a function of the event amplitude A: (a) for ACT-2 and (b) for ACT-3.

According to the simulation results of TeV primary protons [16], the sensitive radius of the telescope should be 150 m, corresponding to an area of $7 \times 10^8 cm^2$. If the FWHM of the decoherence curve is taken as the effective field of view, the effective solid angle of ACT-2 and ACT-3 is 6.9×10^{-4}sr. When the telescope was fixed pointing to the zenith during a term of 588 min, 5888 events were obtained with amplitudes greater than 0.1 V. In this case, 99% of recorded events are induced by the VHE primary protons. The integrated flux of cosmic rays was estimated to be 3.5×10^{-7}/cm · s · sr, which corresponds to the primary protons with energy above 9 TeV. Because of the efficiency producing Cherenkov radiation for gamma-rays is greater than that for protons by a factor of 3, when η_r is 98%, it corresponds to a threshold energy of 3 TeV for gamma-rays. The threshold voltage of 30 mV of the discriminator corresponds to a lowest detectable energy of VHE gamma-rays of the telescope, which is about 1 TeV. In this case the relative integrated efficiency is about 70%.

4. CONCLUSION

Comparing the test results of the performance with other similar telescopes [13-15,17], we found that the main performance of our telescopes is as good as theirs, to some extent it is even better. Of course, as the first generation of Cherenkov telescopes, it has its intrinsic defects. For example, it cannot distinguish between gamma-ray-induced showers and proton-induced showers, and it holds a higher detection threshold energy and a lower flux sensitivity. The periodic VHE gamma-rays of the Crab Nebula and the distribution of the VHE gamma-ray intensity near the galactic plane have been observed in the more than six months of operation, and some interesting results have been obtained. In order to enhance the significance of observation results, we must accumulate more data from a longer term of observation. An alternative is to decrease the threshold energy of the telescope. There are two possible methods to decrease the threshold. One is to use some kind of filter sheet mounted at the front of PM's cathode. Some groups have filtered off 70% of the night background and maintained 70% of Cherenkov photons passing through. The second method is that the mirror is front-coated with an aluminum layer to avoid the absorption of the Cherenkov light in the glass. In this way, the average reflection coefficient can be enhanced to a value as high as 0.8-0.9. If the two methods are used simultaneously, the threshold energy could be expected to decrease by a factor of 0.5.

ACKNOWLEDGMENT

We would like to express our thanks to Prof. He Zhehui for her continuous encouragement and help.

REFERENCES

[1] T.C. Weekes, *Phys. Rep.*, **160**(1988), p. 1.
[2] T.C. Weekes, *Space Sci. Rev.*, **59**(1992), p. 315.
[3] J.W. Cronin *et al.*, *Ann. Rev. Nucl. Part. Sci.*, **43**(1993), p. 883.
[4] A.I. Gibson *et al.*, *Proc. Int. Workshop on VHE γ-Ray Astronomy, Dotacamund, India, 1982.*
[5] K.E. Turver, *Very High Energy Gamma-Ray Astronomy*, Durham, UK 1986.
[6] P. Fleury and G. Vacanti, *Proc. "Towards a Major Atmospheric Cherenkov Detector," Palaiseau, France, 1992.*
[7] T.C. Lamb, *Proc. "Towards a Major Atmospheric Cherenkov Detector-II," Calgary, Canada, 1993.*
[8] T. Kifune, *Proc. "Towards a Major Atmospheric Cherenkov Detector-III," Tokyo, Japan, 1994.*
[9] B.B. Raubenheimer *et al.*, *Proc. "Towards a Major Atmospheric Cherenkov Detector-II," Calgary, Canada, 1993*, p. 3.

[10] R.C. Lamb., *Proc. "Towards a Major Atmospheric Cherenkov Detector-III," Tokyo, Japan* (1994), p. 11.
[11] M. Punch *et al.*, *Nature*, **258**(1992), p. 477.
[12] M. Schubnell *et al.*, *Proc. "Towards a Major Atmospheric Cherenkov Detector-III," Tokyo, Japan* (1994), p. 91.
[13] A.I. Gibson *et al.*, *Proc. Int. Workshop on VHE γ-ray Astronomy, Dotacamund, India* (1982), p. 97.
[14] R.C. Lamb *et al.*, *Proc. Int. Workshop on VHE γ-ray Astronomy, Dotacamund, India* (1982), p. 86.
[15] R. Koul *et al.*, *J. Phys. E. Sci. Instum.* (printed in the UK), **22**(1989), p. 47.
[16] E. Krys and A. Wasilewski, *Proc. "Towards a Major Atmospheric Cherenkov Detector-II," Calgary, Canada* (1993), p. 199.
[17] H.I. De Jager *et al.*, *S. Afr. J. Phys.*, **9**(1986), p. 107.